

Cite this: *Polym. Chem.*, 2024, **15**,  
3063Received 4th February 2024,  
Accepted 29th June 2024

DOI: 10.1039/d4py00141a

rsc.li/polymers

# Low dielectric polymers at high frequency with bulky adamantane groups as the linker†

Leyao Zhao, Jing Sun\* and Qiang Fang \*

Two monomers with adamantane units as the linker and benzocyclobutene (BCB) groups as the cross-linking units have been successfully synthesized, and they are thermally treated to form polymers with a 5% weight loss temperature of up to 478 °C and a glass transition temperature of more than 350 °C. Among the polymers, the one containing fluorobenzene units displays a dielectric constant ( $D_k$ ) of 2.58 and a dielectric loss ( $D_f$ ) of  $1.94 \times 10^{-3}$  at a frequency of 10 GHz. Such a fluoro-containing polymer also exhibits a water uptake of 0.12% even when immersing it in boiling water for 72 h. These results demonstrate that the two polymers are suitable as low dielectric materials for application in the fabrication of devices used in high-frequency communication.

## Introduction

Nowadays, with the continuous advancement of modern communication technology, electronic devices are being developed towards miniaturization, densification, high frequency and high speed. Inevitably, crosstalk and resistance/capacitance (RC) delay occur during the process of signal transmission.<sup>1–5</sup> Therefore, low dielectric materials with a dielectric constant ( $D_k$ ) < 2.6 and low dielectric loss ( $D_f$ ) <  $2.0 \times 10^{-3}$  are urgently needed to eliminate the deterioration of signal transmission in the GHz band. As the dielectric interlayers or substrate resins of printed circuit board (PCB), low dielectric materials are required to have outstanding thermostability, high hydrophobicity, and excellent mechanical properties besides low  $D_k$  and  $D_f$ .<sup>6,7</sup> Among conventional dielectric materials, epoxy resins,<sup>8,9</sup> cyanate esters,<sup>10,11</sup> and polyimides<sup>12,13</sup> display good thermostability; however, they usually possess a  $D_k$  value of above 3.0 and a  $D_f$  value of around 0.01. Although polytetrafluoroethylene (PTFE) has a  $D_k$  value of 2.0–2.2, the processability and thermostability need to be improved.<sup>14</sup> Therefore, achieving low dielectric materials with excellent comprehensive properties is still challenging.

Thermosetting benzocyclobutene (BCB)-based resins have been considered as promising low dielectric materials due to

their high thermostability, good mechanical strength and a convenient curing process without any extra initiators.<sup>15,16</sup> A BCB-based resin called DVS-BCB has been commercialized by Dow Chemical Company, which displays a  $D_k$  value of 2.65 at a frequency of 1 MHz.<sup>17,18</sup> Although it shows good comprehensive properties, the dielectric performance needs to be improved for ongoing requirements of high frequency communication technology. In order to obtain BCB-based resins with better dielectric performance, various research studies have been carried out. In principle, there are two effective methods to reduce the  $D_k$  of organic materials.<sup>19,20</sup> One is to introduce the least polarizable groups, *e.g.*, C–H, C–C, C–F, and C–Si bonds.<sup>21–23</sup> The other is to decrease the dipole numbers by increasing the free volume or porosity.<sup>24–26</sup> Considering that the introduction of too many pores may cause the issue of decreasing mechanical properties or increasing water absorption of materials, the incorporation of bulky groups with large free volume is often employed to decrease the  $D_k$  value of materials. In this context, Shen *et al.* introduced a rosin-based phenanthrene hydride ring into benzocyclobutene (BCB) resin, and found that the increased free volume can effectively reduce the  $D_k$  value of the resin.<sup>27</sup> In addition, the incorporation of low polarity fluorinated groups with bulky groups can be regarded to further decrease  $D_k$ . Among the bulky groups, adamantane units have been highly regarded because of their rigid bulky skeletons and high thermal stability.<sup>28</sup> Xiao *et al.*<sup>29</sup> and our group<sup>30</sup> reported low- $k$  polymers by incorporating both the rigid adamantane and perfluorocyclobutyl groups. The combined effects of bulky and low polarity groups lead to low  $D_k$  of materials ( $D_k < 2.30$ ). However, the procedure for the synthesis of molecules with adamantane units and fluoro groups is usually complicated. This inspires us to develop a

Key Laboratory of Fluorine and Nitrogen Chemistry and Advanced Materials, Shanghai Institute of Organic Chemistry, CAS, 345 Lingling Road, Shanghai 200032, China. E-mail: qiangfang@sioc.ac.cn, sunjing@sioc.ac.cn; Fax: +86 21 54925337; Tel: +86 21 54925337

† Electronic supplementary information (ESI) available: <sup>1</sup>H NMR and <sup>13</sup>C NMR spectra of compound AB and <sup>1</sup>H NMR, <sup>13</sup>C NMR, and <sup>19</sup>F NMR spectra of monomer AFB as mentioned in the text (PDF). See DOI: <https://doi.org/10.1039/d4py00141a>



facile route to synthesize low dielectric materials with both adamantane and fluoro groups.

In this work, we report two BCB-based monomers with the adamantane group (**AB** and **AFB**). The monomer **AFB** contains both adamantane and fluoro groups. The monomers have been converted to thermo-cross-linked polymers, which display excellent thermostability, high hydrophobicity and good dielectric properties. Because of the coupling effects of the fluorinated group and the adamantane group, cured **AFB** shows a high 5% weight loss temperature of 478 °C and glass transition temperature of over 350 °C, a low  $D_k$  value of 2.58 and a  $D_f$  value of  $1.94 \times 10^{-3}$  at a frequency of 10 GHz. The outstanding comprehensive properties suggest that it is suitable to be applied as a dielectric material in the microelectronics industry. Here, we report the details.

## Experimental section

### Materials

4-Bromobenzocyclobutene was purchased from Chemtarget Technologies Co., China. 1,3-Adamantanediol was obtained from Shanghai D&B Biological Science and Technology Co., Ltd. Palladium acetate and cuprous iodide were purchased from Shanghai Bide Pharmatech Co., Ltd. Pentafluorobenzene and tri-*tert*-butylphosphine tetrafluoroborate were obtained from Shanghai Aladdin Biochemical Technology Co., Ltd. **M1**,<sup>31</sup> **5FBCB**<sup>32</sup> and ligand L (*N1,N2*-bis(thiophen-2-ylmethyl)oxalamide)<sup>33</sup> were prepared by the routes previously reported. All solvents were used as received unless otherwise stated.

### Measurements

<sup>1</sup>H NMR, <sup>13</sup>C NMR and <sup>19</sup>F NMR spectra were obtained on a Mercury 400 MHz NMR or a Bruker 500 MHz NMR spectrometer with CDCl<sub>3</sub> as the solvent. Elemental analysis (EA) was performed on an Elementar VARIO ELIII analyzer. Fourier transform infrared (FTIR) spectra were recorded on a Nicolet 380 spectrometer with KBr pellets. High resolution mass spectra (HRMS) were measured on a Thermo Scientific Q Exactive HF Orbitrap-FTMS with the AP-MALDI positive ion mode. Differential Scanning Calorimetry (DSC) was performed with a DSC Q200 instrument at a heating rate of 10 °C min<sup>-1</sup> under a nitrogen atmosphere. Thermogravimetric analysis (TGA) was performed on Netzsch TG 209F1 apparatus under a nitrogen flow and at a heating rate of 10 °C min<sup>-1</sup>.  $D_k$  and  $D_f$  values were detected using an Agilent n5227a at a frequency of 10 GHz.  $D_k$  and  $D_f$  at a frequency range of 1–10 MHz were analyzed using a 4294A Precision Impedance Analyzer using the capacitance method at room temperature. The contact angle of water was characterized using JC2000C apparatus at room temperature. The glass transition temperature ( $T_g$ ) and storage modulus were determined using a DMA Q800 instrument under a nitrogen flow at a heating rate of 5 °C min<sup>-1</sup>. The coefficient of thermal expansion (CTE) was measured on a DIL 402 Expedit instrument and the heating rate was 5 °C min<sup>-1</sup> under a nitrogen atmosphere. X-ray diffraction (XRD) was investigated with a PANalytical X'Pert Powder instrument.

### Synthesis of monomer AB

To a mixture of **M1** (10.00 g, 31.21 mmol), sodium ascorbate (2.50 g, 12.48 mmol), ligand L (1.75 g, 6.24 mmol), Cs<sub>2</sub>CO<sub>3</sub> (40.70 g, 124.84 mmol), and CuI (1.19 g, 6.24 mmol) was added a solution of 4-bromobenzocyclobutene (12.57 g, 68.66 mmol) in DMF (150 mL). The mixture was stirred, heated to 150 °C and kept at that temperature for 4 h. After cooling to room temperature, the mixture was filtered, and the filtrate was concentrated under reduced pressure and the residue was purified by flash column chromatography using hexane as the eluent. The obtained crude product was recrystallized from tetrahydrofuran to give **AB** as a white solid (8.00 g, a yield of 49%). <sup>1</sup>H NMR (500 MHz, CDCl<sub>3</sub>)  $\delta$  (ppm) 7.32 (d,  $J$  = 8.6 Hz, 4H), 6.99 (d,  $J$  = 7.9 Hz, 2H), 6.93 (d,  $J$  = 7.9 Hz, 4H), 6.86 (d,  $J$  = 7.9 Hz, 2H), 6.75 (s, 2H), 3.19–3.06 (m, 8H), 2.31 (s, 2H), 2.00 (s, 2H), 1.94 (d,  $J$  = 3.0 Hz, 8H), 1.78 (s, 2H). <sup>13</sup>C NMR (126 MHz, CDCl<sub>3</sub>)  $\delta$  (ppm) 156.66, 156.03, 146.81, 145.18, 140.42, 126.18, 123.90, 118.51, 117.99, 114.43, 49.57, 42.51, 36.99, 35.95, 29.70, 29.18, 29.05. HRMS-MALDI ( $m/z$ ): Calcd for C<sub>38</sub>H<sub>36</sub>O<sub>2</sub> [M]<sup>+</sup> 524.2712. Found, 524.2710. Anal. Calcd for C<sub>38</sub>H<sub>36</sub>O<sub>2</sub>: C, 86.90; H, 6.92; Found: C, 86.99; H, 6.92.

### Synthesis of monomer AFB

A mixture of **M1** (5.00 g, 15.60 mmol), **5FBCB** (8.85 g, 32.76 mmol), anhydrous K<sub>2</sub>CO<sub>3</sub> (6.47 g, 46.80 mmol), benzyl triethylammonium chloride (TEBAC) (0.36 g, 1.56 mmol), and DMSO (150 mL) was stirred at 60 °C in N<sub>2</sub> for 10 h. After cooling to room temperature, the resulting mixture was filtered, and the filtrate was poured into water (200 mL) and extracted with ethyl acetate (2 × 100 mL). The organic phase was combined, washed with saturated aq. NaCl solution, and dried over anhydrous Na<sub>2</sub>SO<sub>4</sub>. The organic solution was concentrated under reduced pressure. The residue was purified by flash column chromatography using hexane as the eluent. Pure **AFB** was obtained as a white solid (11.67 g, a yield of 91%). <sup>1</sup>H NMR (500 MHz, CDCl<sub>3</sub>)  $\delta$  (ppm) 7.37 (d,  $J$  = 8.6 Hz, 4H), 7.29 (d,  $J$  = 7.7 Hz, 2H), 7.20 (d,  $J$  = 7.6 Hz, 2H), 7.15 (s, 2H), 7.00 (d,  $J$  = 8.4 Hz, 4H), 3.31–3.21 (m, 8H), 2.33 (s, 2H), 2.01 (s, 2H), 1.95 (d,  $J$  = 3.0 Hz, 8H), 1.79 (s, 2H). <sup>13</sup>C NMR (126 MHz, CDCl<sub>3</sub>)  $\delta$  (ppm) 155.42, 147.26, 146.27, 146.11, 145.58–145.32 (m, 2C), 143.60–143.36 (m, 2C), 143.10–142.80 (m, 2C), 141.11–140.79 (m, 2C), 132.65 (t,  $J$  = 13.2 Hz, 2C), 129.04, 126.40, 125.30, 124.40, 123.02, 117.84 (t,  $J$  = 17.2 Hz, 2C), 115.35, 49.40, 42.42, 37.04, 35.85, 29.85, 29.76, 29.63. <sup>19</sup>F NMR (376 MHz, CDCl<sub>3</sub>)  $\delta$  (ppm) –130.65 (dd,  $J$  = 23.0, 9.4 Hz, 4F), –141.41 (dd,  $J$  = 22.6, 9.5 Hz, 4F). HRMS-MALDI ( $m/z$ ): Calcd for C<sub>50</sub>H<sub>40</sub>O<sub>2</sub>NF<sub>8</sub> [M + NH<sub>4</sub>]<sup>+</sup> 838.2932. Found, 838.2926. Anal. Calcd for C<sub>50</sub>H<sub>36</sub>F<sub>8</sub>O<sub>2</sub>: C, 73.11; H, 4.59; F, 18.40; Found: C, 73.16; H, 4.42; F, 18.52.

### Preparation of the cured sheets

Monomer **AB** (about 1.3 g) was added to a flat bottom glass tube with a diameter of 3 cm. The tube was heated to 160 °C in an oil bath in N<sub>2</sub> until the monomer melted. The temperature was further raised to 220 °C and the temperature was



maintained for 3 h. Thus, a pre-cured sheet was formed, which was then placed in a quartz tube furnace, and the temperature of the furnace was maintained at 220 °C for 2 h, 250 °C for 1.5 h, and 270 °C for 1 h, respectively. The cured **AB** sheet was hence obtained, which was used for the measurement of dielectric properties and water absorption. Similarly, a cured **AFB** sheet was prepared.

### Fabrication of the cured films for water contact angle measurement

A solution of monomer **AB** (95 mg, 0.18 mmol) in mesitylene (1.0 mL) was heated to 200 °C and maintained at this temperature for 4 h with vigorous stirring. Thus, a pre-polymer solution was obtained. For the preparation of the film, the pre-polymer solution was spun onto the surface of a silicon wafer. The silicon wafer was placed in a quartz tube furnace, and the temperature of the furnace was maintained at 200 °C in N<sub>2</sub> for 1 h and 210 °C for 1 h, respectively. The obtained cured film on a silicon wafer was used for water contact angle testing. The cured **AFB** film on the silicon wafer was prepared using a similar procedure.

### Measurement of water absorption

The cured **AB** and **AFB** sheets were immersed in 200 mL of boiling water for the set time, and then taken out of water. The weights of the sheets were measured after removing the residual water on the surface of the sample by using filter paper. Water absorption of a sheet was calculated using weight change according to the formula  $W_C (\%) = (M - M_0)/M_0$ , where  $M$  and  $M_0$  were the weight of the sheet after immersion in water and the initial weight, respectively. The final data were obtained from the average of the results of five samples.

## Results and discussion

### Synthesis and characterization

The synthesis routes of monomer **AB** and monomer **AFB** are shown in Scheme 1. **M1** was prepared by a Friedel–Crafts alkyl-

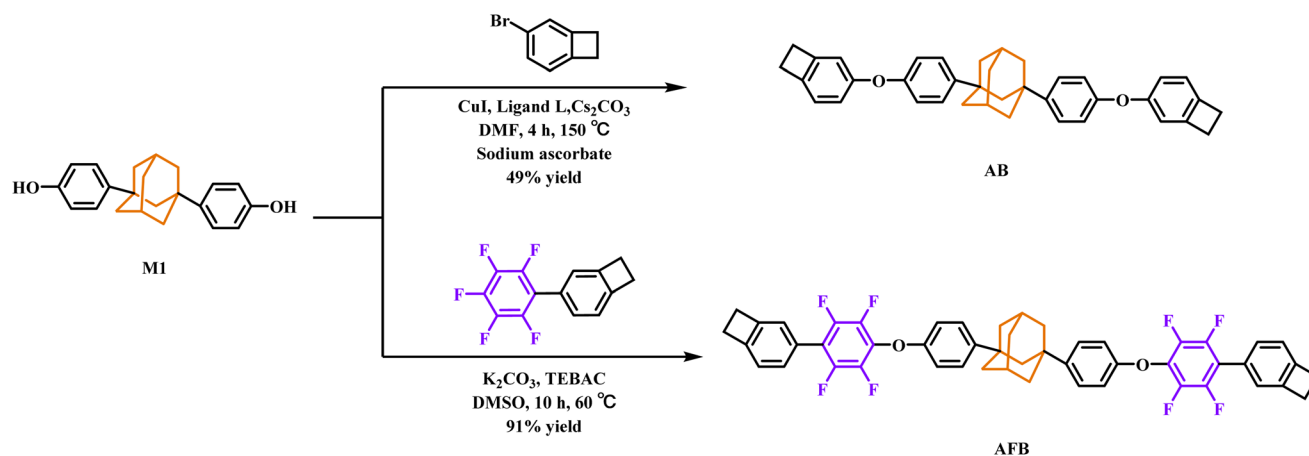
ation reaction between 1,3-adamantanediol and phenol. The monomer **AB** was synthesized from **M1** and 4-bromobenzocyclobutene through the Ullmann–Ma reaction. The monomer **AFB** was prepared from **M1** and **5FBCB** by aromatic nucleophilic substitution in a high yield of 91%.

The chemical structures of **AB** and **AFB** were characterized by <sup>1</sup>H NMR, <sup>19</sup>F NMR and <sup>13</sup>C NMR, HR-MS, FT-IR and elemental analysis (EA). As shown in the <sup>1</sup>H NMR spectra of **AB** and **AFB** (Fig. S1 and S3 in the ESI†), the peaks at 3.27 ppm correspond to the characteristic protons of the methylene group of benzocyclobutene. The signals at 2.4–1.7 ppm are attributed to the protons of adamantane units. All the results confirm that the monomers are successfully synthesized as the proposed structures.

### Thermo-crosslinking reaction of the monomers

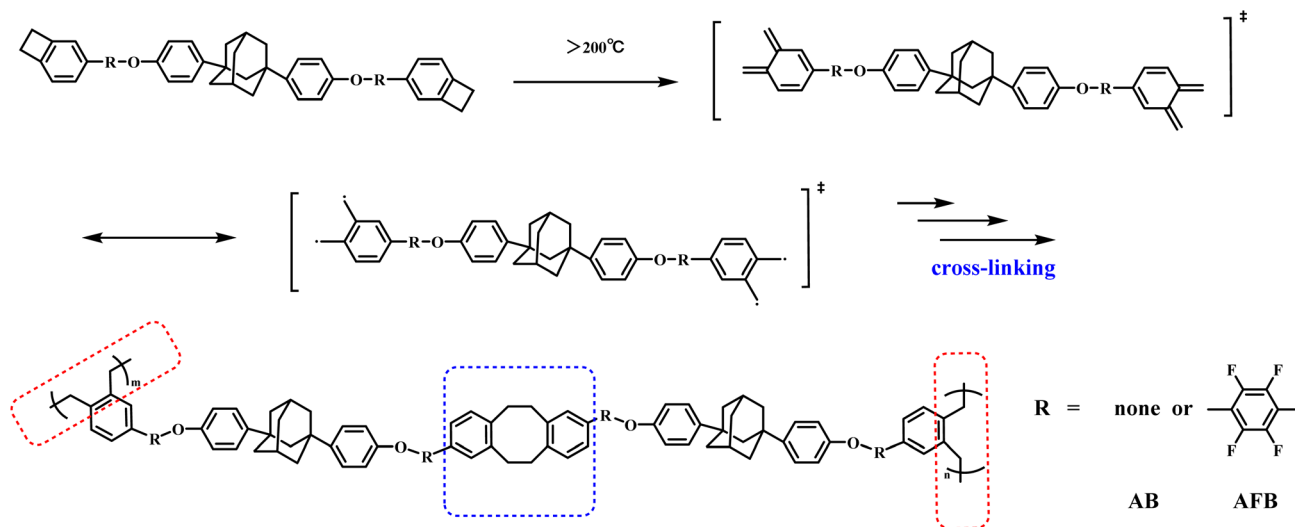
Because of the high reactivity of the benzocyclobutene group at high temperature, monomers **AB** and **AFB** can be thermally cured, and the proposed curing mechanism is illustrated in Scheme 2. During heating, the quaternary ring of benzocyclobutene produces o-quinone dimethane intermediates, which can form eight-membered rings *via* the [4 + 4] cycloaddition reaction or polystyrene fragments by homopolymerization. Thus, monomers **AB** and **AFB** can be converted to thermally cross-linked polymers.

The curing behaviors of **AB** and **AFB** were monitored by differential scanning calorimetry (DSC), and the results are shown in Fig. 1. From the first scans traced by solid lines, **AB** and **AFB** display a melting point of 163 °C and 132 °C, respectively. Both the monomers show the onset curing temperature at about 192 °C and the maximum exothermic peak appears at around 261 °C. The curing behaviors are in accordance with those of the reported BCB-based resins.<sup>34</sup> There is no exothermic peak that can be observed in the second scans traced by the dashed lines, indicating that the monomers have been cured completely. Compared to monomer **AB**, the lower melting point of **AFB** gives it a wider processing window.



**Scheme 1** The procedure for the synthesis of **AB** and **AFB** monomers.





**Scheme 2** A proposed schematic of the curing reaction of AB and AFB.

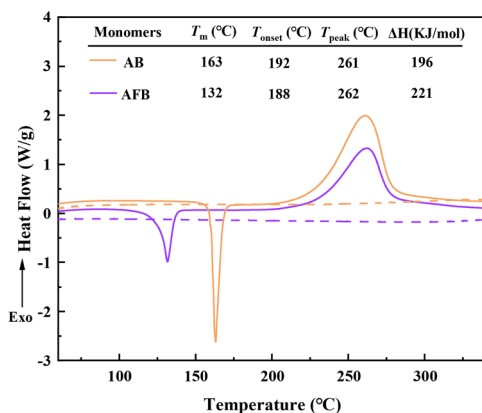


**Fig. 1** DSC traces of AB and AFB at a heating rate of  $10^{\circ}\text{C min}^{-1}$ .

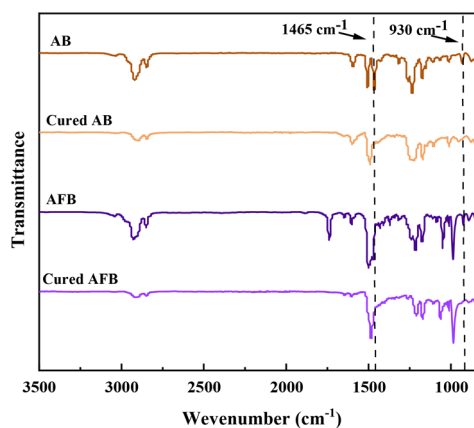


**Fig. 2** FT-IR spectra of AB, AFB, cured AB and cured AFB.

The curing reactions of AB and AFB were further investigated by FT-IR spectroscopy. Comparing the FT-IR spectra of the monomers shown in Fig. 2, it was found that the characteristic BCB absorption peaks at  $930\text{ cm}^{-1}$  and  $1465\text{ cm}^{-1}$  disappeared after curing. It demonstrates that the conversion of monomers into cross-linked polymers has been completed.

### Thermostability

Thermostability is an important parameter to evaluate the performance of dielectric materials. The thermostability of cured AB and cured AFB was detected by thermo-gravimetric analysis (TGA). According to the results shown in Fig. 3, both cured AB and cured AFB display high 5% weight loss temperatures ( $T_{5d}$ ) of  $475^{\circ}\text{C}$  and  $478^{\circ}\text{C}$ , respectively. Cured AFB has a higher char yield (60.9%) than cured AB (23.8%). The results are better than many of the reported BCB-based polymers, indicating that the polymers have excellent thermostability.

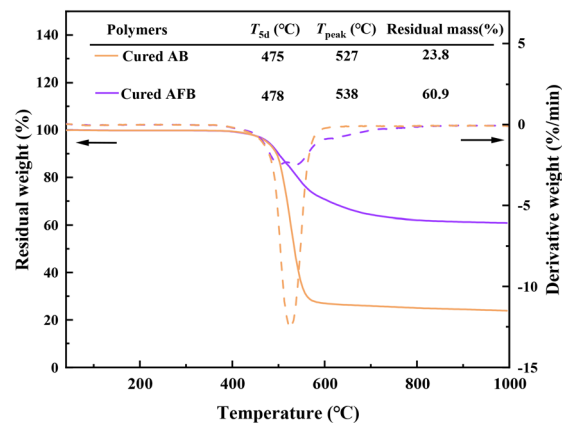


**Fig. 3** TGA curves of AB and AFB at a heating rate of  $10^{\circ}\text{C min}^{-1}$  under  $\text{N}_2$ .



The thermal-mechanical properties of the cured polymers were analyzed by dynamic thermomechanical analysis (DMA). The DMA curves in Fig. 4 show that cured **AB** and cured **AFB** have storage moduli of 0.98 GPa and 1.62 GPa at room temperature, respectively. Based on the peak of  $\tan \delta$ , the  $T_g$  of cured **AB** and cured **AFB** are determined to be 359.4 °C and 380.9 °C, respectively. The high  $T_g$ s of polymers indicate that they can tolerate high-temperature processing for the fabrication of microelectronic devices.

The thermal dimension stability is a critical feature to evaluate the reliability of the polymers at high temperature, which can be determined using the coefficient of thermal expansion (CTE). The CTEs were measured and the results are shown in Fig. 5. The cured **AB** and cured **AFB** display CTEs of 43.3 ppm °C<sup>-1</sup> and 56.6 ppm °C<sup>-1</sup> in the temperature range of 25–300/280 °C, respectively, which are lower than those of most of the BCB-based resins in a wide temperature range.<sup>35</sup> It indicates that cured **AB** and cured **AFB** have good thermal dimension stability.

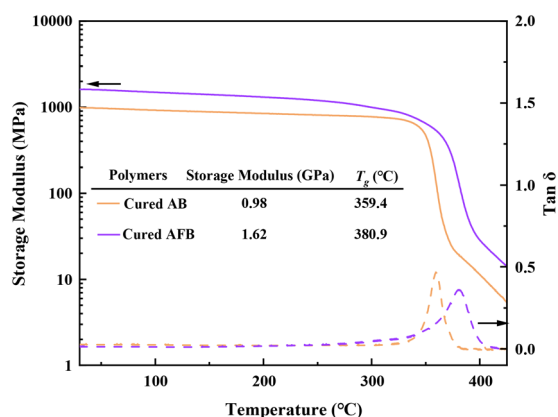


Fig. 4 DMA curves of cured **AB** and cured **AFB** at a heating rate of 5 °C min<sup>-1</sup> in N<sub>2</sub>.

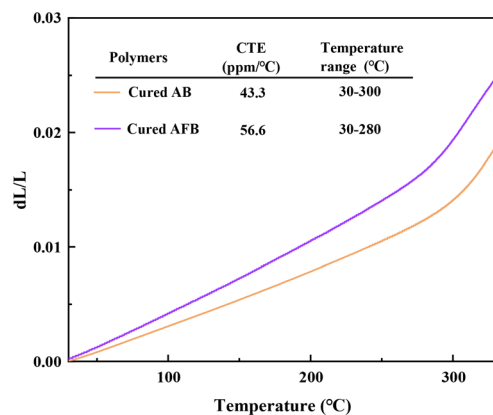


Fig. 5 CTE curves of cured **AB** and cured **AFB** at a heating rate of 5 °C min<sup>-1</sup> in N<sub>2</sub>.

## Dielectric properties

$D_k$  and  $D_f$  are the key parameters to assess the performance of dielectric materials. Low  $D_k$  and  $D_f$  are conducive to improving the speed and quality of signal transmission for high-frequency communication technology. The  $D_k$  and  $D_f$  of cured **AB** and cured **AFB** were measured by using a split post dielectric resonator method at a frequency of 10 GHz and a capacitance method at a frequency ranging from 1 to 10 MHz, respectively. For comparison, a BCB-based resin derived from bisphenol A (BPA-BCB) was synthesized and cured, and the  $D_k$  and  $D_f$  of cured BPA-BCB were measured by the same method. According to Table 1 and Fig. S6,† cured **AB** has a  $D_k$  value of 2.71 @ 10 GHz and a  $D_k$  value of 2.72 @ 1 MHz, which are lower than those of cured BPA-BCB ( $D_k = 2.79$  @ 10 GHz;  $D_k = 2.80$  @ 1 MHz).<sup>36</sup> It demonstrates that the bulky adamantane group can increase the free volume that is beneficial for lower  $D_k$ . Cured **AFB** has a  $D_k$  value of 2.58 and a  $D_f$  value of  $1.94 \times 10^{-3}$  @ 10 GHz and a  $D_k$  value of 2.58 and a  $D_f$  value of  $1.56 \times 10^{-3}$  @ 1 MHz. Relative to cured **AB**, cured **AFB** displays lower  $D_k$  and  $D_f$ , which can be attributed to the introduction of the fluorinated group. Reducing molecular polarizability is conducive to decreasing the  $D_k$  and  $D_f$  values. Compared to the reported thermosetting resins containing fluorobenzene groups (as shown in Table 2), the cured **AFB** displayed better low dielectric properties. It can be ascribed to the combined effects of adamantane and fluorinated groups.

The difference in the dielectric properties between two molecules may be caused by the introduction of fluorobenzene which increases the distance between the molecular chains of the cured resin and thus increases the free volume. In order to investigate the free volume of the two cured monomers, powder X-ray diffraction (XRD) was carried out and the results are shown in Fig. 6. From the figure, it can be seen that the  $2\theta$  angle of the cured **AB** is larger at 16°, while the  $2\theta$  angle of the cured **AFB** is smaller at 14.9°. Based on the XRD data, the distances between the molecular chains of cured **AB** and cured **AFB** were calculated using the Bragg equation (eqn (1)). The molecular chain distances were obtained to be 0.554 nm for cured **AB** and 0.651 nm for cured **AFB**. Thus, the cured **AFB** has a larger free volume, which results in a lower dielectric constant of cured **AFB**.

$$2d \sin \theta = n\lambda \quad (1)$$

Table 1  $D_k$  and  $D_f$  values of the cured polymers at 10 GHz

Polymers	$D_k$	$D_f$
Cured <b>AB</b>	2.71	$2.77^a$
Cured <b>AFB</b>	2.58	$2.61^a$
Cured BPA-BCB	2.79	$3.13 \times 10^{-3}$

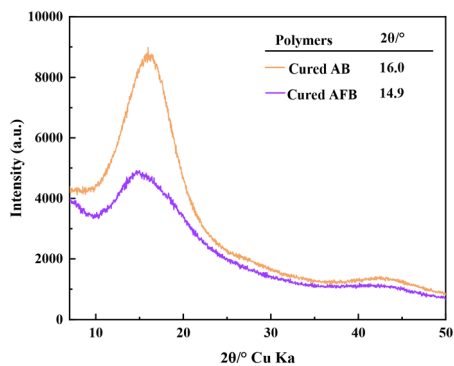
<sup>a</sup> Measured after samples were soaked in boiling water for up to 72 h.





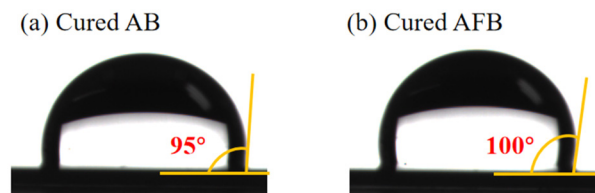
**Table 2**  $D_k$  and  $D_f$  values of the reported resins containing fluorobenzene

Entry	$D_k$	$D_f$	Frequency	$T_{5d}$ (°C)	Ref.
1	~3.0	$3 \times 10^{-3}$	0.15–30 MHz	—	39
2	2.80	$5.29 \times 10^{-3}$	5 GHz	439	40
3	2.60	$1.40 \times 10^{-3}$	10 GHz	483	32
4	2.89	$6.1 \times 10^{-3}$	10 GHz	468	13
5	2.61	$2.60 \times 10^{-3}$	10 GHz	447	41
This work	2.58	$1.94 \times 10^{-3}$	10 GHz	478	—

**Fig. 6** X-ray diffraction patterns of cured **AB** and cured **AFB**.

### Hydrophobicity

High hydrophobicity is important for dielectric materials to prevent deterioration of performance by moisture.<sup>37,38</sup> The hydrophobicity of the polymers is characterized by the contact angle of water on the surface of the polymer film on a silicon wafer. As shown in Fig. 7, the contact angles of cured **AB** and cured **AFB** are 95° and 100°, respectively.

**Fig. 7** The contact angles of water on the surface of (a) cured **AB** and (b) cured **AFB**.

The hydrophobicity of cured **AB** and cured **AFB** was also investigated by measuring the water absorption. The polymer sheets were immersed in boiling water for 72 h. The water absorption was tested every 24 h. After 72 h, the water absorption of cured **AB** and cured **AFB** is low at 0.27% and 0.12% (shown in Table 3), respectively. Compared to the polymer without the adamantane group,<sup>36</sup> low water absorption of cured **AB** and cured **AFB** indicates that both polymers have good hydrophobicity that is attributed to the introduction of the adamantane group. Because of possessing a fluorinated group, cured **AFB** display better hydrophobicity with a higher contact angle and lower water uptake relative to cured **AB**.



**Table 3** Water uptake (%) of the cured **AB** and cured **AFB** after immersion in boiling water

Polymers	24 h	48 h	72 h
Cured <b>AB</b>	0.16	0.27	0.27
Cured <b>AFB</b>	0.02	0.12	0.12

Additionally, the dielectric behaviors of cured sheets after immersing in boiling water were investigated. The  $D_k$  and  $D_f$  values of cured **AB** increased slightly after immersing, whereas those of cured **AFB** did not significantly change (Table 1). The introduction of fluorine atoms into the cured **AFB** enhances the surface hydrophobicity and decreases water absorption. Hence, it helps to prevent water from permeating the polymer sheets to maintain low  $D_k$  and  $D_f$ .

## Conclusion

In summary, two BCB-containing monomers **AB** and **AFB** with adamantane groups were synthesized from adamantanediol by a facile method. The monomers were cured by treating them at high temperatures. The cured polymers displayed high thermostability, good hydrophobicity and low dielectric properties. Cured **AFB** containing both fluorinated and adamantane groups exhibited excellent comprehensive properties with a low  $D_k$  value of 2.58 and a  $D_f$  value of  $1.94 \times 10^{-3}$  at 10 GHz, a  $T_g$  value of over 380 °C and a low CTE of 56.6 ppm °C<sup>-1</sup> in the temperature range of 25–280 °C. It indicates that the resins are appropriate for utilization as dielectric substrates or packaging materials for high-frequency communication applications.

## Author contributions

Leyao Zhao: synthesis, investigation, data collection, and writing – original draft. Jing Sun: supervision and writing – review & editing. Qiang Fang: supervision, conceptualization, and writing – review & editing.

## Data availability

This manuscript was completed with the personal contributions of all authors. All data are available.

## Conflicts of interest

The authors declare no competing financial interests.

## Acknowledgements

Financial support from the National Natural Science Foundation of China (NSFC, No. 22075311 and 22175195), the

Strategic Priority Research Program of the Chinese Academy of Sciences (Grant No. XDB0590000) and the Science and Technology Commission of Shanghai Municipality (23ZR1476200) is gratefully acknowledged.

## References

- G. Maier, *Prog. Polym. Sci.*, 2001, **26**, 3–65.
- D. Shamiryan, T. Abell, F. Iacopi and K. Maex, *Mater. Today*, 2004, **7**, 34–39.
- W. Volksen, R. D. Miller and G. Dubois, *Chem. Rev.*, 2010, **110**, 56–110.
- L. Wang, C. Liu, S. Shen, M. Xu and X. Liu, *Adv. Ind. Eng. Polym. Res.*, 2020, **3**, 138–148.
- X. Zhang, Y. Zhang, Q. Zhou, X. Zhang and S. Guo, *Ind. Eng. Chem. Res.*, 2020, **59**, 1142–1150.
- J. Hou, J. Sun and Q. Fang, *Eur. Polym. J.*, 2022, **163**, 110943.
- J. Hou, J. Sun and Q. Fang, *Chin. J. Chem.*, 2023, **41**, 2371–2381.
- Y. Wu, X. Fan, Z. Wang, Z. Zhang and Z. Liu, *Polym. Adv. Technol.*, 2024, **35**, e6241.
- H. Yang, G. Yuan, E. Jiao, K. Wang, W. Diao, Z. Li, Z. Liu, K. Wu and J. Shi, *ACS Appl. Polym. Mater.*, 2024, **6**, 1116–1128.
- J.-Y. Shieh, S.-P. Yang, M.-F. Wu and C.-S. Wang, *J. Polym. Sci., Polym. Chem.*, 2004, **42**, 2589–2600.
- Y. Zhou, Z. Zhang, P. Wang and X. Ma, *Composites, Part A*, 2022, **162**, 107136.
- R. Bei, C. Qian, Y. Zhang, Z. Chi, S. Liu, X. Chen, J. Xu and M. P. Aldred, *J. Mater. Chem. C*, 2017, **5**, 12807–12815.
- Y. Feng, J. Sun and Q. Fang, *ACS Appl. Polym. Mater.*, 2023, **5**, 4419–4426.
- G. J. Puts, P. Crouse and B. M. Ameduri, *Chem. Rev.*, 2019, **119**, 1763–1805.
- J. Hou, L. Fang, G. Huang, M. Dai, F. Liu, C. Wang, M. Li, H. Zhang, J. Sun and Q. Fang, *ACS Appl. Polym. Mater.*, 2021, **3**, 2835–2848.
- T. Huang, X. Zhang, T. Wang, H. Zhang, Y. Li, H. Bao, M. Chen and L. Wu, *Nano-Micro Lett.*, 2023, **15**, 14–24.
- J. Yang, Y. Cheng and F. Xiao, *Eur. Polym. J.*, 2012, **48**, 751–760.
- Q. Peng, J. Ma, J. Wu, R. Chen, Z. Pu, J. Zhong and J. Yang, *Polym. Chem.*, 2023, **14**, 3446–3452.
- Z. Hu, X. Liu, T. Ren, H. A. M. Saeed, Q. Wang, X. Cui, K. Huai, S. Huang, Y. Xia, K. Fu, J. Zhang and Y. Chen, *J. Polym. Eng.*, 2022, **42**, 677–687.
- M. Xie, M. Li, Q. Sun, W. Fan, S. Xia and W. Fu, *Mater. Sci. Semicond. Process.*, 2022, **139**, 106320.
- J. Wang, J. Zhou, K. Jin, L. Wang, J. Sun and Q. Fang, *Macromolecules*, 2017, **50**, 9394–9402.
- X. Chen, J. Sun, L. Fang, Y. Tao, X. Chen, J. Zhou and Q. Fang, *ACS Appl. Polym. Mater.*, 2020, **2**, 768–774.
- F. Liu, J. Sun and Q. Fang, *ACS Appl. Polym. Mater.*, 2022, **4**, 842–848.



- 24 A. Jain, S. Rogojevic, S. Ponoth, N. Agarwal, I. Matthew, W. N. Gill, P. Persans, M. Tomozawa, J. L. Plawsky and E. Simonyi, *Thin Solid Films*, 2001, **398–399**, 513–522.
- 25 D. J. Michalak, J. M. Blackwell, J. M. Torres, A. Sengupta, L. E. Kreno, J. S. Clarke and D. Pantuso, *J. Mater.*, 2015, **30**, 3363–3385.
- 26 J. Wang, J. Sun, J. Zhou, K. Jin and Q. Fang, *ACS Appl. Mater. Interfaces*, 2017, **9**, 12782–12790.
- 27 F. Fu, M. Shen, D. Wang, H. Liu, S. Shang, F.-L. Hu, Z. Song and J. Song, *Biomacromolecules*, 2022, **23**, 2856–2866.
- 28 Y. Cheng, W. Chen, Z. Li, T. Zhu, Z. Zhang and Y. Jin, *RSC Adv.*, 2017, **7**, 14406–14412.
- 29 L. Kong, T. Qi, Z. Ren, Y. Jin, Y. Li, Y. Cheng and F. Xiao, *RSC Adv.*, 2016, **6**, 68560–68567.
- 30 L. Fang, J. Zhou, C. He, Y. Tao, C. Wang, M. Dai, H. Wang, J. Sun and Q. Fang, *Polym. Chem.*, 2020, **11**, 2674–2680.
- 31 M. Frank, L. Gregor, K. Karsten, WO2019/141833 A1, 2019.
- 32 H. Zhang, J. Sun and Q. Fang, *Eur. Polym. J.*, 2022, **179**, 111527.
- 33 Y. Chen, S. Li, L. Xu and D. Ma, *J. Org. Chem.*, 2023, **88**, 3330–3334.
- 34 G. Huang, R. Shi, J. Sun and Q. Fang, *Eur. Polym. J.*, 2023, **196**, 112310.
- 35 R. A. Kirchhoff, C. J. Carriere, K. J. Bruza, N. G. Rondan and R. L. Sammler, *J. Macromol. Sci., Part A: Pure Appl. Chem.*, 1991, **28**, 1079–1113.
- 36 X. Zuo, X. Zhao, B. Liu, S. Yang and L. Fan, *J. Appl. Polym.*, 2009, **112**, 2781–2791.
- 37 P. Marx, A. J. Wanner, Z. Zhang, H. Jin, I.-A. Tsekmes, J. J. Smit, W. Kern and F. Wiesbrock, *Polymers*, 2017, **9**, 195.
- 38 R. Bei, K. Chen, Y. He, C. Li, Z. Chi, S. Liu, J. Xu and Y. Zhang, *J. Mater. Chem. C*, 2023, **11**, 10274–10281.
- 39 F. He, C. Yuan, K. Li, S. Diao, K. Jin, J. Wang, J. Tong, J. Ma and Q. Fang, *RSC Adv.*, 2013, **3**, 23128–23132.
- 40 M. Dai, J. Sun and Q. Fang, *Polym. Chem.*, 2022, **13**, 4484–4489.
- 41 F. Liu, M. Li, J. Sun and Q. Fang, *Biomacromolecules*, 2023, **24**, 4819–4830.

